Journal of Zhejiang University-SCIENCE A (Applied Physics & Engineering)
ISSN 1673-565X (Print); ISSN 1862-1775 (Online)
www.zju.edu.cn/jzus; www.springerlink.com
E-mail: jzus@zju.edu.cn

Tidal current turbine based on hydraulic transmission system*

Hong-wei LIU†, Wei LI, Yong-gang LIN†‡, Shun MA

(*State Key Laboratory of Fluid Power Transmission and Control, Zhejiang University, Hangzhou 310027, China*)

†E-mail: zju000@163.com; yglin@zju.edu.cn

Received July 12, 2010; Revision accepted Mar. 2, 2011; Crosschecked June 21, 2011

Abstract: Tidal current turbines (TCTs) are newly developed electricity generating devices. Aiming at the stabilization of the power output of TCTs, this paper introduces the hydraulic transmission technologies into TCTs. The hydrodynamics of the turbine was analyzed at first and its power output characteristics were predicted. A hydraulic power transmission system and a hydraulic pitch-controlled system were designed. Then related simulations were conducted. Finally, a TCT prototype was manufactured and tested in the workshop. The test results have confirmed the correctness of the current design and availability of installation of the hydraulic system in TCTs.

Key words: Tidal current turbines (TCTs), Hydraulic power transmission, Hydraulic pitch-controlled system, Workshop test
doi:10.1631/jzus.A1000334 **Document code:** A **CLC number:** TH122; TK79; TH137

1 Introduction

The consumption of the energy is rapidly increasing with the industrialization of developing countries. The rising price of oil in recent years and the problems caused by excessive use of the traditional fuel make it urgent to exploit the renewable energy. More and more countries around the world are beginning to spend much time and money on the renewable energy (Pelc and Fujita, 2002; Islam *et al.*, 2004; Richard, 2004), such as wind, ocean, and solar energies. In the recent years, China government has given more supports to promote the utilization of renewable energy sources, in which the tidal current energy was put in a prominent position.

Tidal current turbines (TCTs) are newly developed devices, which are used to capture the kinetic energy of the tidal current and convert it into electricity. Many projects have been undertaken so far and some prototypes have been tested or in testing successfully (Liu *et al.*, 2011), such as the Seaflow (300 kW, 2003, UK Devon, MCT Company) (Fraenkel, 2001; 2004), the Blue project (300 kW, 2003, Norway Hammerfest, Strøm/Statoil/ABB) (Stone, 2003), and the SeaGen (1.2 MW, installed in Mar., 2008, Strangford Lough of Northern Ireland, MCT), and the Roosevelt Island Tidal Energy (RITE) Project (35 kW, started at Dec., 2006, East River of New York, Verdant Power Company USA, and six-unit demonstration array for RITE Project was completed in May, 2007). In China, research on the tidal current energy was started in the 1980s at Harbin Engineering University (HER) and the research was mainly focused on the vertical axis tidal turbine, such as Wanxiang II (40 kW, 2005, HER, China). The study of horizontal axis tidal turbine started in the last five years, was conducted firstly by Zhejiang University and subsequently by the Ocean University of China and Northeast Normal University. The current technology in China is not as advanced as that of many other western countries. In 2010, with the support of the Ocean Energy Special Funds, more corporations are now researching the tidal energy utility, such as China National Offshore Oil Corporation, China Energy Conservation and Environmental Protection Group,

---

‡ Corresponding author
* Project supported by the National Natural Science of China (Nos. 50505043 and 50735004), and the National High Tech R&D Program (863) of China (No. 2007AA05Z443)

China Datang Corporation, Huaneng New Energy Industrial Co., Ltd., and Harbin Electric Corporation.

Because of the harsh marine environment, there are many key problems to be solved for the development of TCTs (Bahaj and Myers, 2003), such as power stability, optimization of turbine blades, structural modal analysis, sealing of the system, and components erosion. This paper focuses only on the power stability of TCTs. The hydraulic transmission and pitch-controlled technologies have been added to the system. Firstly, the hydrodynamics of TCTs was analyzed and the expected power output characteristic of TCTs was given. Then a hydraulic power transmission system and a hydraulic pitch-controlled system were introduced in detail. The simulation results in AMESim and Matlab/Simulink were presented. Finally, a 20 kW prototype was manufactured and used in the workshop to test the theoretical design and the availability of the hydraulic system in TCTs.

2 Hydrodynamics of tidal current turbines

A TCT system is similar to a wind turbine and mainly consists of a turbine, power transmission system and generator attached to the pitch-controlled system, and support foundation, etc. When water flows through the turbine, it forces the turbine to rotate, and then the rotation motion is transmitted to the generator through the power transmission system-gearbox or hydraulic system. In order to study the power performance, the hydrodynamics of the turbine should be analyzed first.

2.1 Momentum theory and blade element theory

Blades are the key components of the TCT, and decide the efficiency of the turbine used to capture ocean energy. Here the captured energy behavior of the turbine has been analyzed based on momentum theory and blade element theory.

From Fig. 1, in the stream-tube, supposing the water is incompressible, according to Bernoulli's equation (Hou *et al.*, 2006) $\rho v^2/2+\rho gz+p=c$, where ρ is the water density, v is the velocity, z is the height, g is gravitational acceleration, p is the pressure, and c denotes a constant, the energy equations of upstream and downstream can be expressed as follows (Burton *et al.*, 2001):

$$\rho v_1^2/2+\rho gz+p_\infty=\rho v^2/2+\rho gz+p^+,$$
$$\rho v_2^2/2+\rho gz+p_\infty=\rho v^2/2+\rho gz+p^-,$$
$$\text{thus, } \rho v_1^2/2-\rho v_2^2/2=p^+-p^-,$$

where v_1 and v_2 are the velocities of the upstream and downstream, respectively; p^+ and p^- are the pressures before and behind the turbine, respectively.

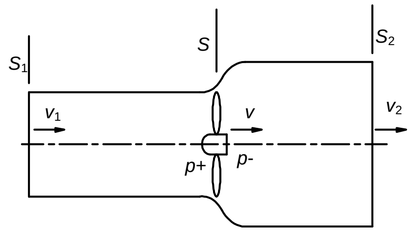

Fig. 1 Stream-tube model of the turbine
S, S_1: swept areas of the turbine; S_2: expanded area of stream tube; v: stream velocity through the turbine

The force acted on the turbine disc is

$$F=(p^+-p^-)S_1=(v_1^2-v_2^2)\rho S_1/2. \quad (1)$$

This force causes the momentum change of water across the turbine, which is equal to $\rho S_1 v(v_1-v_2)$.

According to momentum theory,

$$F=\rho S_1 v(v_1-v_2), \quad (2)$$

let $v_2=av_1$, where a is the axial flow induction factor, and combine Eqs. (1) and (2),

$$v=(v_1+v_2)/2\,.$$

The power extracted from the water is given by

$$P_{\text{capture}}=m_1v_1^2/2-m_2v_2^2/2=C_\text{p}\rho S_1 v_1^3/2, \quad (3)$$

where m_1 and m_2 are the water masses at S_1 and S_2, respectively, and C_p=(1+a)^2(1−a)/2, which presents the power coefficient.

Let $\frac{\mathrm{d}C_\text{p}}{\mathrm{d}a}=0$, and then a=1/3, so we obtain the maximum power extraction coefficient 16/27, and the optimal power P_opt in Fig. 2. However, the maximum power extraction requires the rotation speed of the turbine to be controlled, which will be analyzed as follows.

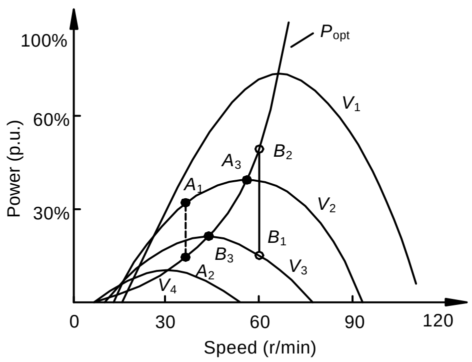

V_1, V_2, V_3, and V_4 denote different velocities, A_2, A_3, B_3, and B_2 are the optimal operation points, and A_1 and B_1 deviate from the optimal power track

Fig. 2 Power performance of the turbine

Fig. 3 shows the forces acting on a blade airfoil, from which these formulae can be drawn as follows (Ye, 2002):

$$
\begin{aligned}
&\mathrm{d}F_{\mathrm{D}} = \frac{1}{2}\rho w^2 l\mathrm{d}r \cdot C_{\mathrm{D}}(i), \\
&\mathrm{d}F_{\mathrm{L}} = \frac{1}{2}\rho w^2 l\mathrm{d}r \cdot C_{\mathrm{L}}(i), \\
&\mathrm{d}F_{\mathrm{t}} = \mathrm{d}F_{\mathrm{L}}\sin(\beta+i) - \mathrm{d}F_{\mathrm{D}}\cos(\beta+i) = \sin(\theta-\xi),
\end{aligned}
\tag{4}
$$

where $\xi = \arctan\dfrac{\mathrm{d}F_{\mathrm{D}}}{\mathrm{d}F_{\mathrm{L}}}$, $\theta=\beta+i$, $w=\sqrt{v^2+(\omega r)^2}$, F_{D} is the drag force, F_{L} is the lift force, F_{t} is the tangent force causing the turbine to rotate, F is the resultant force of F_{D} and F_{L}, C_{D} is the drag coefficient, C_{L} is the lift coefficient, l is the chord, r is the radius of the blade element, β is the fixed angle, ω is the rotational speed of the turbine, and i is the attack angle. AB is the chord length as shown in Fig. 3.

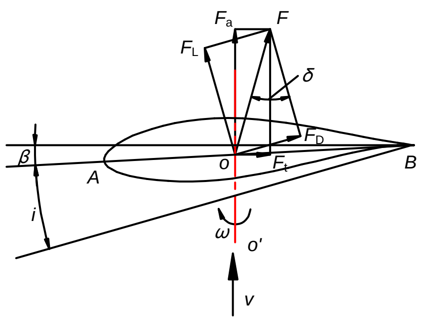

Fig. 3 Analysis of force on blade element

In Eq. (4), θ is a sharp angle, and we hope ξ can be as small as possible in order to obtain a larger F_{t}, so the ratio of $C_{\mathrm{D}}(i)/C_{\mathrm{L}}(i)$ should be as small as possible and an optimal attack angle i_{opt} can be maintained. Also, the wide range of C_{L}, low C_{D}, and delayed stall performance characteristic, should also be specifically noted.

From Fig. 4, the inflow angel $\Phi = \arctan\dfrac{v}{\omega r}$, and $i = \arctan\dfrac{v}{\omega r} - \beta$ can be obtained. When the velocity v changes, the rotation speed ω also needs to be changed to keep an optimal i.

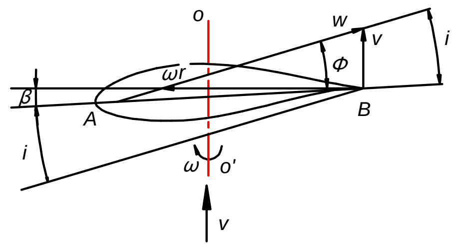

Fig. 4 Blade element velocities

2.2 Power characteristic of tidal current turbines

Since the tidal current velocity varies sinusoidally with the tide cycle, the ideal equipment can produce energy over a wide range of current speeds, although there is a rated running point. With the current speeds changing, the power extraction of the turbine also changes. From Eq. (3), the captured power is proportional to the water velocity of the cube if C_{p} is fixed, but the power cannot exceed the rated power in consideration of the electrical and mechanical structure, so the power extraction characteristic of the turbine should appear as shown in Fig. 5 (starting velocity was taken to be 0.5 m/s).

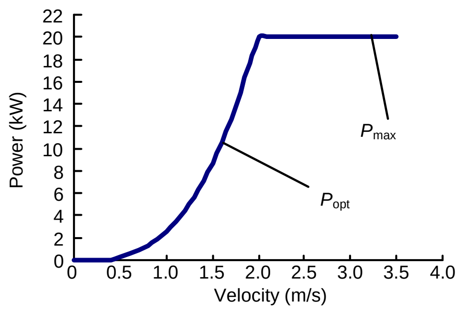

Fig. 5 Expected power output curve of a tidal current turbine

Fig. 6 gives the unit's operational mode at different velocities. In P_{optimal} zone, the turbine should track peak C_{p} and in P_{constant} zone, the power is kept constant around the rated power. As discussed above, when below the rated current speed, in order to maintain the optimum tip-speed ratio or power extraction maximum, the rotor speed should be adjusted in proportion to the water speed v. It is possible to control the load torque at the generator and thus realize the variable speed operation. The method to control the rotor speed through variable displacement pump/motor will be studied later.

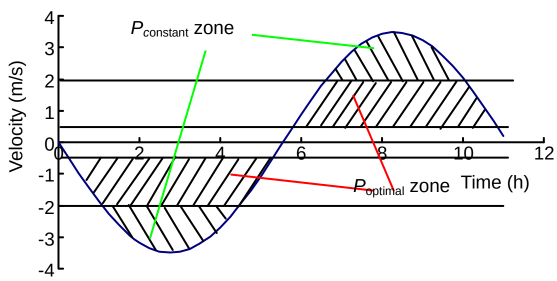

Fig. 6 Operation mode at different velocities

When the current exceeds the rated velocity, pitch control is then used to limit the rotor speed. In this study, the pitch actuator and its hydraulic driven system are designed, simulated, and tested.

3 Hydraulic power transmission of tidal current turbines

3.1 Design of the hydraulic system

High turbine speed can cause some disadvantages for the rotor design, such as increased difficulty of seal design, inducing large noise, and causing cavitations. In order to eliminate these problems, the turbine rotation speed needs to be controlled. However, ordinary generator speed is always above 200 r/min. There must be a drive train system to accelerate the turbine speed to satisfy the request of the generator. Unlike the traditional gearbox power train, here a hydraulic transmission system was chosen. Compared with the gearbox, a hydraulic transmission system has several advantages. Firstly, the turbine torque fluctuation caused by the variation of water speed is usually very large and therefore it is better to use some soft drive train systems to alleviate this fluctuation. Secondly, it affords the power for the hydraulic pitch system described later. Thirdly, displacement-type speed control of a hydraulic motor can be used to adjust the turbine speed enabling the turbine to capture as much energy as possible. Finally, the electrical equipment was simplified when using a hydraulic motor to keep the generator speed constant. Fig. 7 gives the configuration of the hydraulic system: the parts surrounded by a dashed line are the power transmission system, and the other parts are for the hydraulic pitch control.

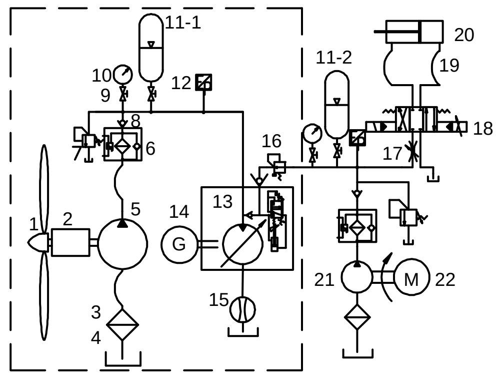

1: turbine; 2: gearbox; 3: filter; 4: hydraulic reservoir; 5: pump; 6: fine filter; 7: relief valve; 8: check valve; 9: cut-off valve; 10: manometer; 11: accumulator; 12: pressure sensor; 13: hydraulic motor; 14: generator; 15: flow sensor; 16: pressure relief valve; 17: throttle valve; 18: proportional directional valve; 19: hydraulic hose; 20: cylinder; 21: auxiliary pump; 22: electrical motor. G and M denote generator and electrical motor, respectively

Fig. 7 Configuration of hydraulic power transmission

In order to keep the optimal tip-speed ratio, the turbine speed needs to be controlled, so the variable displacement motor is used for this purpose. When the turbine speed is slower, the displacement of the motor is diminished, and vice versa. This can be seen in the following formulae:

$$p=\frac{T_{\text{hm}}(\omega_{\text{hm}})}{q_{\text{hm}}}=\frac{T_{\text{hm}}\{[\omega_{\text{pump}}q_{\text{pump}}-Q_{\text{Res}}(\Delta p)]/q_{\text{hm}}\}}{q_{\text{hm}}}, \tag{5}$$

$$\dot{\omega}_{\text{turbine}}=\frac{T_{\text{turbine}}-pq_{\text{pump}}}{J_{\text{turbine}}}=\frac{f(\omega_{\text{turbine}},v,\beta)-pq_{\text{pump}}}{J_{\text{turbine}}}, \tag{6}$$

where T_{hm}, ω_{hm}, and q_{hm} are the load torque, speed, and displacement of the hydraulic motor, respectively, p is the pressure of the hydraulic system, ω_{pump} and q_{pump} are the speed and displacement of the pump, respectively, $Q_{\text{Res}}(\Delta p)$ is the flow of the accumulator, and ω_{turbine}, $\dot{\omega}_{\text{turbine}}$, T_{turbine}, and J_{turbine} are the speed, acceleration, torque, and moment of inertia of the turbine, respectively. q_{pump} and β are taken to be fixed and $T_{\text{hm}} \propto \omega_{\text{hm}}$. $f(\omega_{\text{turbine}}, v, \beta)$ is the function of ω_{turbine}, v, and β.

Fig. 8 is a photo of the completed hydraulic system, where two accumulators were used, one for the hydraulic power train system, and the other for the hydraulic pitch-controlled system.

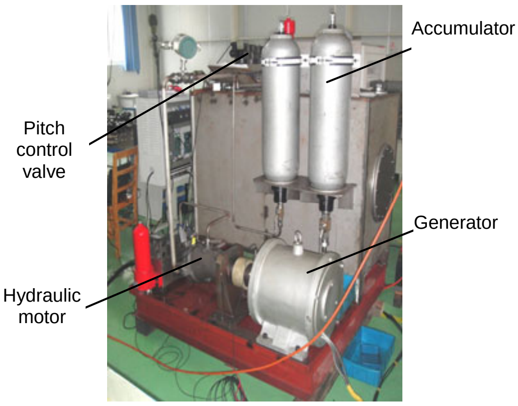

Fig. 8 Photo of hydraulic system

3.2 Performance of the hydraulic power train

In order to study the performance of the hydraulic power train, numerical simulation was undertaken using Matlab/Simulink and AMESim (Fig. 9). In the simulation, the water velocity data are transmitted from the external file to the turbine subsystem, and a look-up table is used to present the turbine hydrodynamics performance. The hydraulic power train system model was built in AMESim, and is embedded in Fig. 9 in the form of s-function.

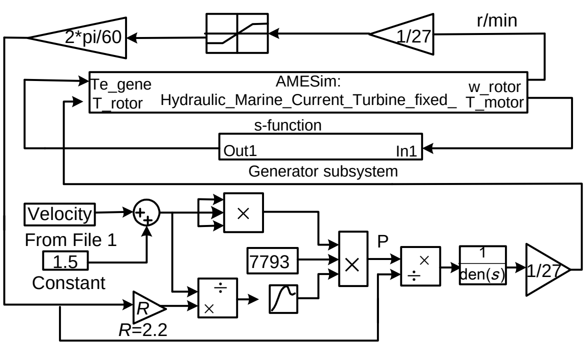

Te_gene: electromagnetic torque; T_rotor: turbine torque; w_rotor: rotary speed of the pump; T_motor: driven torque of generator; *R*: radius of turbine; P: power

Fig. 9 Simulation model in Matlab/Simulink

Fig. 10a presents the simulation results. It can be seen that the turbine power is almost identical to the pump power which is approximately 20 kW and the output power of hydraulic motor is 15 kW, so the efficiency of the hydraulic power train is approximately 75%. Compared to the efficiency of a gearbox which is always above 90%, although the efficiency of the hydraulic transmission system is lower, the power output becomes flatter and the succeeding electrical equipment would be simplified. This can be explained according to Fig. 11, which presents the flows of the pump, hydraulic motor, and accumulator in the simulation.

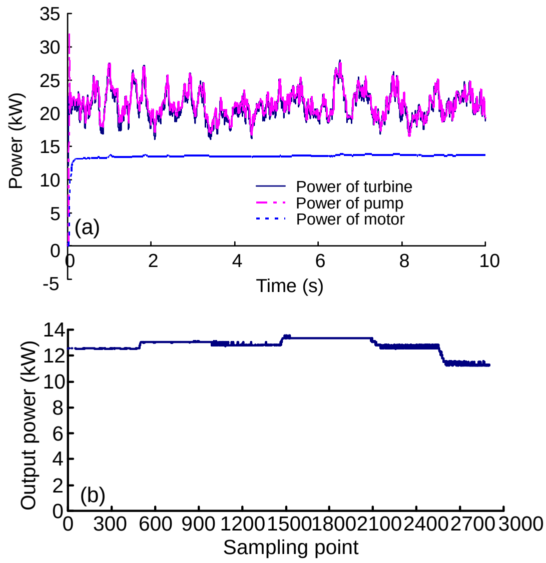

Fig. 10 Results of the simulation and tests

(a) Simulated power of the pump, motor, and turbine; (b) Power output results in tests

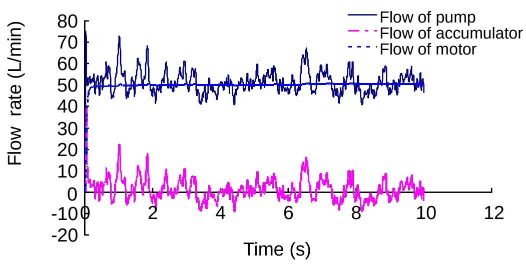

Fig. 11 Flows of pump, hydraulic motor, and accumulator

The equipment was tested in workshop. In the tests, a controllable electrical motor was used instead of a turbine, and a three-phase permanent synchronous generator was adopted. Also, damp loads and storage battery were used to consume the generated power. The damp loads were switched on or off according to the voltage of storage battery. The test data were recorded by the computer through an RS232 serial port. Fig. 10b gives the output power of the workshop test, and the output power is approximately 13 kW and is smaller than that of the simulation, which can be attributed to the deviation from the rated operational conditions during the tests.

The efficiencies of the hydraulic power train are discussed as follows. In the experiments, the pressure and flow of the hydraulic power train, and the electrical power, were measured. The total efficiency of the hydraulic and electrical systems can be obtained, which is the ratio of electrical power and the hydraulic input power, and the efficiency is above 70%. Furthermore, the efficiency can be improved to some extent by the optimization of the hydraulic pipeline layout (Lin *et al.*, 2008). The 30% loss is attributed to the mechanical efficiency of the hydraulic components, and the leakage, etc., and will appear as heat, which is an important problem for a tidal turbine. However, during the operation of the tidal turbine at sea, because the pump is below the water surface and the motor is above the water, there will be some oil pipes immersed in the sea water, and this would partially cool the oil. With the dimensions of oil pump and valve port enlarged in the large full-scaled turbine, the power loss will be decreased.

4 Pitch-controlled system of tidal current turbines

4.1 Pitch actuator

A pitch-controlled system or a yaw drive is needed for a horizontal axis turbine to operate in a bi-directional tidal current. In this study, the pitch-controlled system is selected, and Fig. 12 gives the structure of a pitch actuation system, which used a rack and pinion gearing. The rack was driven by a hydraulic cylinder and engaged with the gear which was coupled to the blades by bolts.

For the pitch-controlled system, the demand of rapid response is not very high because of the predictability and periodicity of the water current. So an electro-hydraulic proportional direction valve was selected to control the blade rotation direction, and an accumulator was used to maintain the hydraulic pressure. Also, a throttle valve was used to change the blade pitch speed. Fig. 13 is the photo of the 20 kW full-scaled pitch-controlled system.

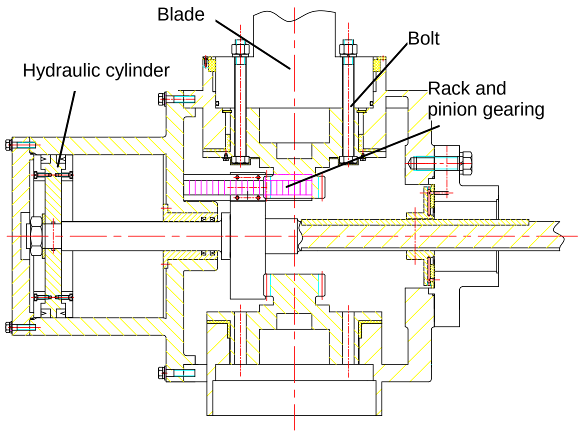

Fig. 12 Pitch actuation system

Fig. 13 Photo of the pitch system

4.2 Pitch controller and control strategy

When the pitch-controlled system is used as a substitute for the yaw system, it is a position-controlled system and has two demanded values which differ from each other by almost 180°, as shown in Fig. 14 in which the current flow direction was measured on May 11, 2009 (Liu, 2009).

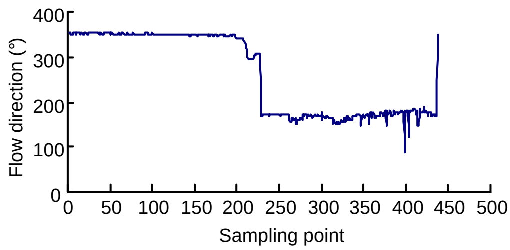

Fig. 14 Measured direction of tidal current

The hydraulic pitch driven system is presented in Fig. 7. An electro-hydraulic proportional direction valve was used to control the flow of oil to the actuator cylinder. The valve opening is set in proportion to the pitch demand. The pitch position demand comes from the turbine controller and is compared with the measured pitch position, and the pitch-position error is transformed into a pitch-rate demand through a proportional-integral-differential (PID) control loop.

An accumulator was used to supply the hydraulic energy temporally when the motor was shut off. Also, a throttle valve was used to change the blade pitch speed.

In the control codes of the pitch system, two methods can be used to deal with the bi-directional flow: the feedback control which was described above, and the sequential control which acts according to the period characteristic of the tide current. At the same time, the pitch system can be used for power control by introducing the power feedback, and shutdown of the turbine by blade feathering and backpaddling, etc.

4.3 Simulations and experiments

The performance of the hydraulic driven pitch-controlled system was simulated in Matlab/Simulink. Fig. 15 is the simulation framework of the pitch-controlled system, where K_a and K_q are the amplification parameter and flow gain of the proportional valve, respectively. $G_{BL}(s)$ is the transfer function of the proportional valve and it can be treated as a two-order oscillation element (Wang, 2006). The controller adopted PID, which was verified to be applicable from the results of simulation and workshop tests.

Fig. 16 gives the simulation and test results of the pitch-controlled system. From the test results, the governing time of the system controlled by PID algorithm is approximately 1 s and the overshoot is zero, which can be attributed to friction and damp. The pressure of the hydraulic pitch system is approximately 3.75 MPa, which was thought primarily to resist the friction force.

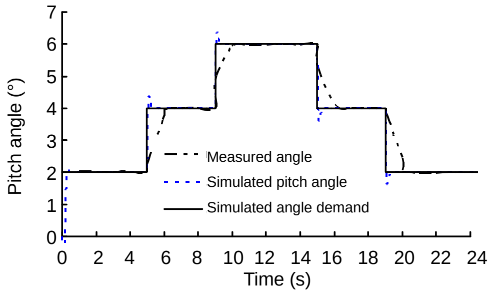

Fig. 16 Results of the pitch-controlled system tests

5 Conclusions and perspectives

This paper studied a hydraulic power system adopted in a TCT, which not only stabilizes the power output, but also allows a TCT to operate at variable rotor speeds to optimize power capture. Thus the efficiency of the rotor is maximized. At the same time, the hydraulic pitch-controlled system can be used for bi-directional flow and power control, etc. When the rated capacity might be exceeded, the hydraulic pitch system can be switched on to maintain the rated output.

A case study based on a 20 kW horizontal axis TCT was undertaken in this paper. The simulation and workshop test results show that the hydraulic

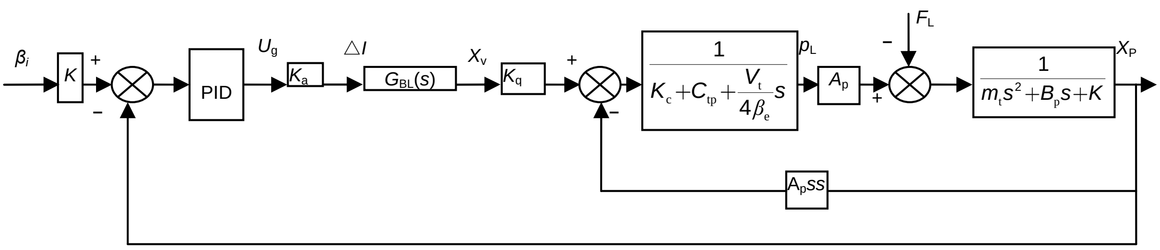

β_i: pitch demand; K: proportion factor; U_g, $\triangle I$: input voltage and control current of the proportional amplifier; X_v: spool displacement; K_q, K_c: slide valve factors; C_{tp}: cylinder leaking factor; V_t: compressed volume of cylinder; β_e: bulk modulus of oil; A_p: piston area; p_L: cylinder pressure; F_L: pitch load; X_P: displacement of cylinder; K, B_P, m_t: elastic coefficient, damp coefficient, and the mass of cylinder

Fig. 15 Simulation framework of the pitch-controlled system

power transmission efficiency exceeds 70%. The performance of the hydraulic pitch system is also investigated, and the results are satisfactory.

Furthermore, a full size system such as 1 MW or larger can be realized in principle based on this work, and some mechanical structures such as the pitch actuator may be improved because of its large space in the hub.

Acknowledgements

The authors are grateful for advice and contributions from Dr. Xiao-jing SUN at Shanghai University, China.

Reference

Bahaj, A.S., Myers, L.E., 2003. Fundamentals applicable to the utilisation of marine current turbines for energy production. *Renewable energy*, **28**(14):2205-2211. [doi:10.1016/S0960-1481(03)00103-4]

Burton, T., Sharpe, D., Jenkins, N., Bossanyi, E., 2001. Wind Energy Handbook. John Wiley & Sons, Ltd., Baffins Lane, Chichester, England. [doi:10.1002/0470846062]

Fraenkel, P., 2001. The tide turns for marine current turbines. *International Water Power & Dam Construction*, **53**(12):18-21.

Fraenkel, P., 2004. Windmills below the sea: a commercial reality soon? *Refocus*, **5**(2):46-48. [doi:10.1016/S1471-0846(04)00111-8]

Hou, G.X., Sun, J.L, Wang, X.Z, Feng, D.K., 2006. Engineering Fluid Mechanics. Mechanics Industry Publishing Company, Beijing, China (in Chinese).

Islam, M., Fartaj, A., Ting, D., 2004. Current utilization and future prospects of emerging renewable energy applications in Canada. *Renewable and Sustainable Energy Reviews*, **8**(6):493-519. [doi:10.1016/j.rser.2003.12.006]

Lin, X., Pan, S.X., Wang, D.Y., 2008. Dynamic simulation and optimal control strategy for a parallel hybrid hydraulic excavator. *Journal of Zhejiang University-SCIENCE A*, **9**(5):624-632. [doi:10.1631/jzus.A071552]

Liu, H.W., 2009. Study on the Key Technologies of Horizontal Axis Marine Current Turbine's Mechanics. PhD Thesis, Zhejiang University, Hangzhou, China (in Chinese).

Liu, H.W., Ma, S., Li, W., Gu, H.G., Lin, Y.G., Sun, X.J., 2011. A review on the development of tidal current energy in China. *Renewable and Sustainable Energy Reviews*, **15**(2):1141-1146. [doi:10.1016/j.rser.2010.11.042]

Pelc, R., Fujita, R.M., 2002. Renewable energy from the ocean. *Marine Policy*, **26**(6):471-479. [doi:10.1016/S0308-597X(02)00045-3]

Richard, B., 2004. The World Offshore Renewable Energy Report 2004-2008. DTI's 2010 Target Team, UK.

Stone, R., 2003. Norway goes with the flow to light up its nights. *Science*, **299**(5605):339. [doi:10.1126/science.299.5605.339]

Wang, C.H., 2006. Hydraulic Control System. Mechanics Industry Publishing Company, Beijing, China (in Chinese).

Ye, H.Y., 2002. Control Technology of the Wind Turbines. Mechanics Industry Publishing Company, Beijing, China (in Chinese).